Materials Research Express

PAPER

Non-destructive control of critical defects and diagnostics of InGaN/GaN heterostructures in power LEDs by using their microplasma characteristics

RECEIVED
16 January 2015

REVISED
20 April 2015

ACCEPTED FOR PUBLICATION
22 April 2015

PUBLISHED
19 May 2015

V P Veleschuk[1], A I Vlasenko[1], Z K Vlasenko[1], M P Kisselyuk[1] and V V Borshch[2]

[1] V. Lashkaryov Institute of Semiconductor Physics, National Academy of Sciences of Ukraine, 41 Nauki Avenue, 03680 Kyiv, Ukraine
[2] Poltava National Technical Yuri Kondratyuk University, 24 Pershotravnevyi Avenue, 36011 Poltava, Ukraine

E-mail: vvvit@ukr.net

Keywords: power LED, InGaN/GaN, avalanche breakdown, non-destructive diagnostics

Abstract

In this work, we studied the controlled microplasma breakdown of InGaN/GaN heterostructures in power light-emitting diodes (LEDs) prepared on various substrates (SiC, AuSn/Si, Al_2O_3). It was ascertained that LED microplasma characteristics are related to their functional parameters. It was shown that nondestructive control of the critical defects and diagnostics of the InGaN/GaN power LEDs are possible because they are based on the following parameters of microplasmas: (1) voltage of the first microplasma; (2) current of the first microplasma; (3) amount of the microplasmas; (4) integrated luminescence intensity of the microplasmas; (5) ratio of the blue and yellow band luminescence peak intensities for the microplasmas; (6) displacement between electroluminescence peaks for forward and reverse biases. It was ascertained that the majority of microplasmas arise near the faces of the crystallites' grain boundaries.

1. Introduction

Today, there is a predominant tendency to fabricate light-emitting diode (LED) heterostructures based on GaN with a large area, and to integrate them in matrices. However, the increase of the area in the epitaxial growth results in more nonuniform distribution of internal mechanical strains and extended defects. The latter increases the probability that 'critical' defects will appear and thus dominate the process of worsening the functional parameters and the reliability of the LEDs [1, 2]. Two urgent problems can arise: the express detection and nondestructive control of these electrically active extended defects (imperfect regions) in InGaN/GaN heterostructures of power LEDs.

In addition to various methods of diagnostics and reliability prognostication based on a diversity of elemental and structural analysis techniques and different electrophysics methods, there also exist methods that are effective in the nondestructive characterization and quality control of GaN (InGaN, AlGaN) structures methods, such as local photo-, electro-, and cathode-luminescence (PL, EL, and CL) [2–5]. Also, we should note the effective method of dark lock-in thermography, because it can be applied to Si solar cells [6].

However, it is not always possible to detect critical electrically active extended defects (defect regions), which dominantly influence the electric and luminescent functional parameters of InGaN/GaN structures.

At the same time, application of a reverse voltage to a GaN structure produces a controlled microplasma (MP) breakdown that takes place mainly in the regions of extended defects and is accompanied by luminescence [1, 4–16]. MPs are localized regions with a high current density of avalanche ionization that are formed due to small structural defects in the depletion region. A strong electric field is created in local areas of the inversely biased p-n junction, and this field is usually accompanied by luminescence. The breakdown avalanche current of the MP is significantly inhomogeneous, with density distribution on the p-n junction area. MPs arise due to either a local increase in electric field strength or an increase in the ionization rate coefficients.

Table 1. Characteristics of the InGaN/GaN heterostructures and MPs.

Parameter	Substrate		
	SiC	AuSn/Si	Al_2O_3
Dislocation density, ρ (cm^{-2})	$\sim 10^7$	$\sim 10^9$	$\sim 10^9$
Luminous flux, Φ (Lm)	30.6	21	15
Voltage of the first MP, U_{1MP} (V)	−29	−23	−18
Current of the first MP, J_{1MP} (μA)	−11	−35	−210
Amount of the MPs on the surface (N_{MP})	27	54	178
Integrated EL intensity of the MP, I_{MP} (a.u.)	1	1.1	1.4
Ratio of the blue band and yellow band EL, $I_{450\ nm}/I_{580\ nm}$	3.5	2.14	2
Displacement, $\Delta\lambda_{MP}$ (nm)	18	20	34

In recent years, MP breakdown was studied in various GaN structures [1, 4–11, 14–16], but it was not studied purposefully in power (I_{nom} = 350…500 mA) InGaN/GaN LEDs grown on different types of substrates. Also, the question of MP sources is open, and these sources have not been studied in detail.

Therefore, the purpose of the paper is to study the features of MPs in InGaN/GaN structures prepared on various substrates from which industrial-power LEDs are made.

2. Experiment

In this work, we investigated industrial InGaN/GaN power LEDs (P_{el} = 1 W, I_{nom} = 350 mA) of blue light (λ_{peak} = 460…470 nm). The heterostructures had an area of 1 mm^2 and were made using MOCVD technology on different substrates, including SiC, Al_2O_3, and structures grown on a sapphire substrate and carried after the laser lift-off process [17] on the Si substrate by means of AuSn (eutectic) contact. The indium content in quantum wells (QW) for all types of heterostructures was identical and equal to x = 0.2.

The EL spectra of the MPs were measured using the spectroradiometer HAAS—2000 (Everfine), with a large integration time for clear detection of spectral lines. Duration of spectral measurements was 5 min. Current-voltage characteristics (CVC) were measured using the constant current.

Table 1 summarizes and represents values such as dislocation density (ρ), light flux (F), and the parameters of the MP breakdown, which are discussed below.

3. Results

Figure 1(a) shows the EL spectra of MPs in InGaN/GaN structures at the reverse biases of U_{rev} = −40 V (1, 2) and U_{rev} = −24 V (3), and at the forward bias (the respective nominal current was 350 mA). For the structure prepared on the Al_2O_3 substrate, the 40 V voltage is unattainable because a destructive breakdown takes place, and the voltage of appearance of the first MP, U_{1MP}, is lower than that for two other types of LEDs. At the reverse bias of 24 V, MPs in structures on the AuSn/Si and SiC substrates are absent. This can be explained by a higher concentration of extended defects in the structure on the Al_2O_3 substrate.

In the MP spectrum, one can observe the main peak of InGaN QWs with the maximum corresponding to the energy of the band gap, E_g, of InGaN and the shoulder near 400 nm (figure 1, spectrum 1 and 2) or the peak (spectrum 3) related to GaN layers close to the QW. The shoulder within the range 390–430 nm corresponds to recombination on donors and/or acceptors in the p- and n- GaN layers. For the structure on the sapphire substrate, the peak intensity at 400 nm exceeds that of the QW. It is indicative of a higher concentration of donor and acceptor levels, which are also related to defects at the InGaN/GaN interfaces, because a greater mismatch of the lattices at the interface epitaxial layer/Al_2O_3 substrate results in a higher concentration of defects (threading dislocations).

Let us introduce and consider the luminescent parameters of MPs. During analysis, the ratio $I_{BLUE\ BAND}/I_{YELLOW\ BAND}$ is widely used. The ratio of the peak intensities for blue luminescence and yellow luminescence bands (EL or PL) can represent the optical quality [2, 3]. The yellow luminescence of MPs in LEDs within the range 2.1–2.3 eV (536 nm–590 nm) is related to the donor and deep acceptor levels caused by some point defects and their complexes [2, 3]. Figure 1(a) shows that the ratio of peak intensities of the blue band (λ = 450 nm) and at λ = 580 nm ($I_{450\ nm}/I_{580\ nm}$) is equal to 2 for structures on the Al_2O_3 substrate, 2.14 for structures on the AuSn/Si substrate, and 3.5 for structures on the SiC substrate. The respective data is presented in table 1. For the

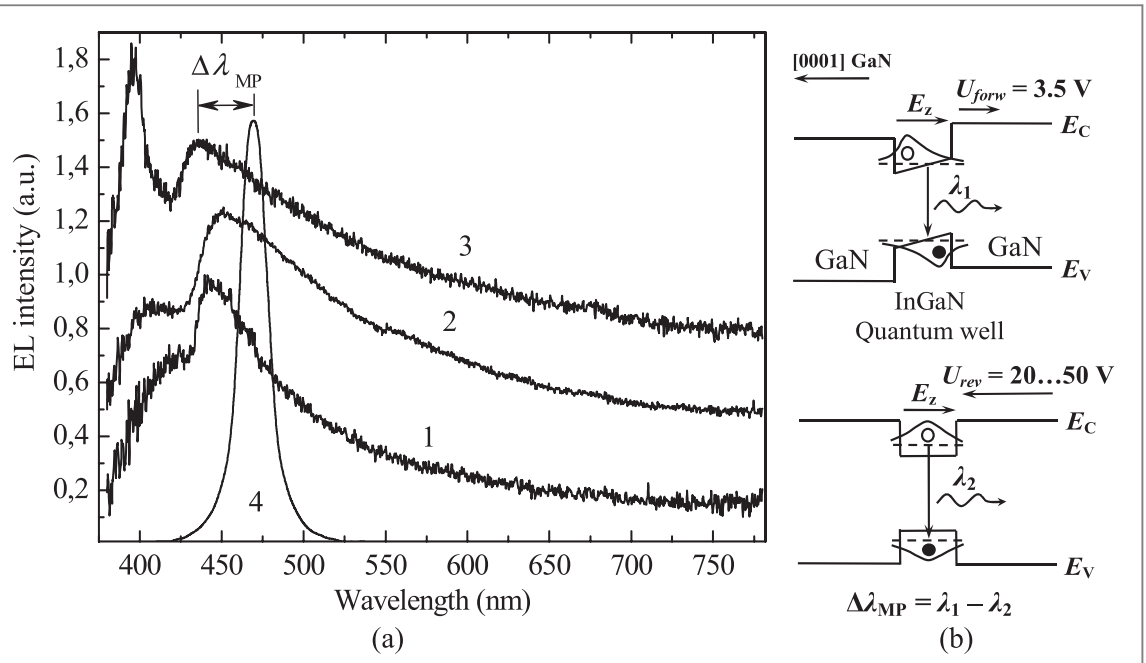

Figure 1. (a) EL spectra of the InGaN/GaN heterostructures at the reverse bias, $U_{rev} = -40$ V (1, 2), −24 V (3), and at the forward bias, $U_{forw} = 3.5$ V, $I = 350$ mA (4). Substrate: (1) SiC, (2) AuSn/Si, and (3, 4) Al_2O_3. (b) Band diagram of the InGaN/GaN heterostructure at the forward, U_{forw}, and reverse, U_{rev}, bias.

structure on the Al_2O_3 substrate, the EL intensity in the yellow band is relatively higher than the intensity of the blue band, in contrast to the other LEDs.

The integrated intensity of the EL inherent to the MP, I_{MP}, is proportional to the reverse current [8, 9] and to the concentration of electrically active defects. It is also related to the quality and reliability of the InGaN/GaN structure [8, 9]. The value of I_{MP} is lowest for the structure on the SiC substrate and highest for the structure on the Al_2O_3 substrate (see table 1).

In figure 1(a), spectrum 4 corresponds to the structure on the Al_2O_3 substrate at the forward bias 3.5 V and current 350 mA (i.e., it is one of the basic parameters for LEDs). Between the peaks of spectra 3 and 4, one can see the interval (displacement) $\Delta\lambda_{MP} = \lambda_1 - \lambda_2$. This blue shift of the EL peak of the InGaN QW during the MP breakdown relative to the EL peak of the QW at forward bias is related to the quantum confined Stark effect in the QW [18, 19]. The blue shift of the peak and value of the displacement, $\Delta\lambda_{MP}$, are determined by and depend on built-in electric fields, $E_z = -P_z/\varepsilon_{GaN}\varepsilon_0$ (figure 1(b)), that arise in the QW due to piezoelectric (P_{PZ}) and spontaneous (P_{SP}) polarizations, $P_z = P_{SP} + P_{PZ}$. Piezoelectric polarization in the vertical direction, in accordance with the expression $P_{PZ} = 2\varepsilon\left[e_{31} - e_{33}(C_{13}/C_{33})\right]$, depends on the component of the strain tensor at the interface $\varepsilon = \varepsilon_{xx} = (a_{substrate} - a_{GaN})/a_{GaN}$. Here, $C_{13\,(33)}$ is the elastic stiffness coefficient of the GaN, and $e_{31\,(33)}$ are the piezoelectric coefficients [18, 19].

Since the heterostructures differ only by substrate material and indium content in the QW (x = 0.2), which are identical for all heterostructures, the displacement, $\Delta\lambda_{MP}$, depends on the value, ε_{xx}, that has the highest meaning for the structure on the Al_2O_3 substrate and the lowest meaning for the structure on the SiC substrate. $\left|\varepsilon_{GaN/SiC}\right| > \left|\varepsilon_{GaN/Al_2O_3}\right|$; the lattice mismatch is 3.3% and 14.8% accordingly.

Being based on the measurements of EL spectra for the forward and reverse voltages, we ascertained that the value $\Delta\lambda_{MP}$ has the highest meaning for the structure placed on the Al_2O_3 substrate and the lowest meaning for the structure on the SiC substrate. The respective data are summarized in table 1.

In addition to the MP luminescence parameters, we also measured parameters of the MP such as the voltage of appearance of the first microplasma (U_{1MP}), the current (J_{1MP}) at which the first MP appears, and the amount of the MP (N_{MP}) at certain voltages. The voltage of appearance of the first MP is indicative of the low threshold inherent to the defect ionization potential, which causes a large leakage current [4, 10]. The amount of luminous MP points, N_{MP}, is proportional to the concentration of dislocations [4]. Results are presented in table 1; the adduced MP parameters were averaged for five LEDs. One can see that N_{MP} and J_{1MP} reach the highest values for the structure on the Al_2O_3 substrate (much higher dislocation concentration) and the lowest values for the structure on the SiC substrate.

In addition to these parameters of the MPs, figure 2 shows the forward and reverse CVC of the heterostructures on various substrates. The value of a tunnel current in the subthreshold region, which is

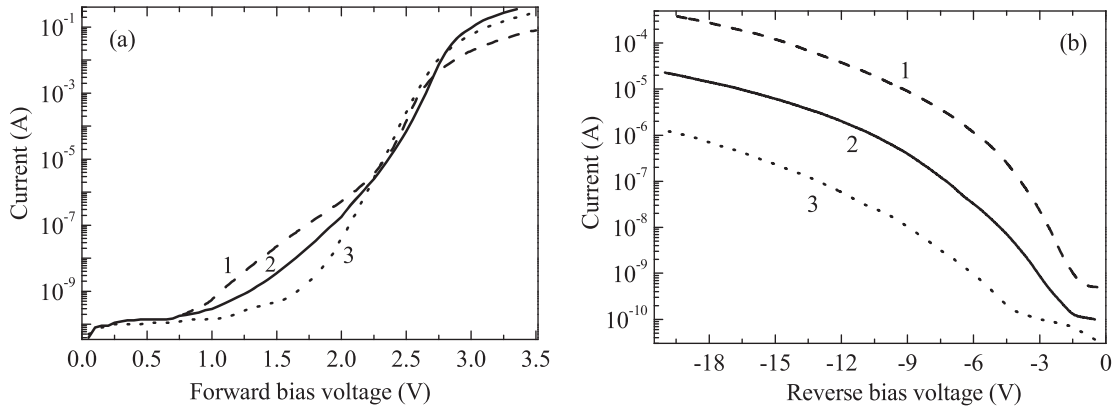

Figure 2. CVC of the InGaN/GaN heterostructures for the (a) forward and (b) reverse bias voltages. (1) On the Al_2O_3, (2) on the AuSn/Si, and (3) on the SiC substrates.

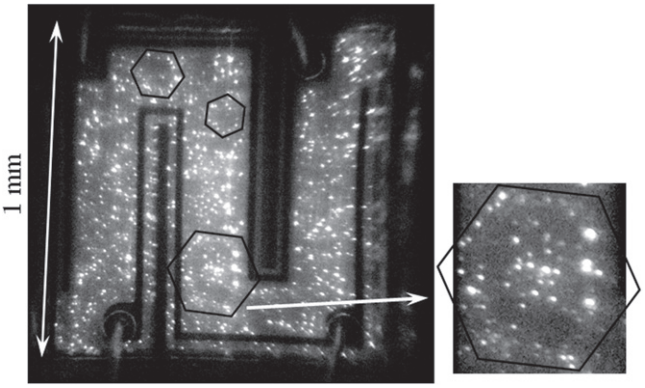

Figure 3. MPs in the InGaN/GaN structure on the sapphire substrate at $U_{rev} = -30$ V, $I_{rev} = 10.8$ mA.

determined by the amount of the extended defects in the depletion region (up to $U_{forw} = 2.2$ V), reaches its maximum in the structure on the Al_2O_3 substrate and its minimum in the structure on the SiC substrate (see figure 2). The highest steepness of the forward CVC is observed in the structure on the SiC substrate, the lowest steepness is inherent to the structure on the Al_2O_3 substrate.

More pronounced differences are observed on the reverse CVC in figure 2(b): The value of the reverse current differs practically by one order for three types of the investigated heterostructures, and this current value is the lowest for the structures on the SiC substrate. This difference in the reverse CVC precisely correlates with the amount of MP points, N_{MP} (see table 1), because extended defects in the depletion region (sources of MP) increase reverse (leakage) and subthreshold currents [11, 20, 21]. It is known that the ratio of the reverse current of two LEDs is proportional to the square of the dislocation densities responsible for the leakage current [20]. The ratio of the current in figure 2 is close to $J_1/J_2 = J_2/J_3 = 20$. The ratio of the $N_{MP1}/N_{MP2} = 3.3$, $N_{MP2}/N_{MP3} = 2$.

To date, the problem of the nature of MPs in epitaxial structures based on GaN and InGaN AlGaN solid solutions is not solved. Sources of the MP in such structures are considered to be threading dislocations [4, 5, 10, 11], clusters of dislocations [1], so-called 'V-shaped defects' [5], or high electric field regions caused by metal contact anomalies [8, 9].

As it was revealed, MPs appear and are clearly pronounced at the grain boundaries of the GaN crystallites, and as it is well known, the grain boundaries are characterized by an enhanced dislocation density. The image of the MPs in the InGaN/GaN structure on the sapphire substrate at $U_{rev} = -30$ V is shown in figure 3. In addition, a selected crystallite of 180 μm is shown, too. Two smaller crystallites are also selected (at the top part). In general, parts of the MPs in figure 3 form lines of the hexagonal structures of crystallites over the whole surface.

At GaN film MOCVD epitaxial growth on the sapphire substrate, hexagonal crystallites are formed with various orientations in the plane of the substrate, with sizes ranging from one to ten micrometers. The film has a mosaic structure [18, 22].

It was ascertained that most MPs arising near the faces of crystallites are located on the crystallites' grain boundaries and appear (switch-on) already at $U_{rev} = -18\ldots20$ V (i.e., they are the low-voltage). Therefore, these MP sources with the lowest switching voltage can be considered to be critical defects.

4. Discussion

As it follows from table 1 and figures 1 and 2, among the three types of investigated LEDs, the heterostructure on the SiC substrate has the lowest density of dislocations (ρ) and the highest value of flux (Φ), maximal values of the U_{1MP}, I_{450}/I_{580}, CVC steepness and the minimal values of J_{1MP}, N_{MP}, I_{MP} and $\Delta\lambda_{MP}$, as well as the lowest values of a tunnel current on forward CVC curve, and especially leakage current on the reverse CVC. On the contrary, the heterostructure on the Al_2O_3 substrate has the highest ρ and the lowest values of flux (Φ), U_{1MP}, I_{450}/I_{580}, CVC steepness, while parameters J_{1MP}, N_{MP}, I_{MP} and $\Delta\lambda_{MP}$ have the highest values. Tunnel and leakage currents at the heterostructure on the Al_2O_3 substrate also have the highest values. The heterostructure on the AuSn/Si substrate has mean values of all the previously mentioned parameters. It has the better parameters than the structure on the Al_2O_3 substrate, because the laser lift-off process was used [17]. In this case, after separation of the structure from Al_2O_3 and transfer onto the SiC substrate by using AuSn eutectics, internal mechanical strains are partially relaxed.

Thus, for the structure on the Al_2O_3 substrate, the parameters of MPs are the most critical among three types of the investigated LEDs. In addition, the EL peak of the MP in the range near 400 nm, which is related to the energy levels on account of defects in GaN, is observed. Also, displacement $\Delta\lambda_{MP}$ between the EL peak of the QW at forward and reverse biases for this structure reaches its maximum, which indicates the greater (integrated) value of the internal mechanical strains.

It ensues from the obtained data that the parameters of MPs summarized in table 1 are related to the luminescent and electric parameters of InGaN/GaN LEDs at the forward (including nominal) bias. For example, at the lowest voltage of MP appearing U_{1MP} and greater currents (both for the first MP, J_{1MP}, and for all reverse CVC), the light flux is less and the dislocation density is large. This result is confirmed by results from [8, 9]. A difference in the MP effects between the Al_2O_3 and SiC substrates is observed by us in [7]. Large leakage currents caused by critical defects lead to faster degradation of LEDs during long-term operation [11].

Thus, the above MP parameters can provide nondestructive express testing of the critical defect regions in the InGaN/GaN heterostructures and additional qualitative control of power LEDs. Quality control is offered for GaN LEDs [7–9], Si solar cells [6, 12], and GaAsP diodes [13].

5. Conclusions

It was shown that nondestructive express testing of the critical defects and diagnostics of the InGaN/GaN power LEDs is possible based on the following parameters of MPs: (1) voltage of the first MP, U_{1MP}; (2) current of the first MP, J_{1MP}; (3) amount of the MPs, N_{MP}; (4) integrated luminescence intensity of MPs, I_{MP}; (5) ratio of the blue and yellow band luminescence peak intensities for MPs, $I_{BLUE\ BAND}/I_{YELLOW\ BAND}$; (6) displacement between electroluminescence peaks for forward and reverse biases, $\Delta\lambda_{MP}$, due to the quantum confined Stark effect.

The luminescent and electric parameters of the MPs for InGaN/GaN power LEDs are related to the InGaN/GaN functional parameters. It is ascertained that among these three investigated heterostructures on the different substrates (SiC, AuSn/Si, Al_2O_3), the heterostructure on the SiC substrate has the best quality and the best functional parameters, in contrast to the heterostructure on the sapphire substrate, which has the highest amount of critical defects.

It was established that the sources of MPs in the InGaN/GaN heterostructures of power LEDs in most cases are corresponding extended defects at the grain boundaries of GaN crystallites.

Acknowledgments

The work was supported by the State Fund for Fundamental Research of Ukraine.

References

[1] Morkoc H 2009 *Handbook of Nitride Semiconductors and Devices: GaN-based Optical and Electronic Devices* vol. 3 (New York: Wiley-VCH) p 898
[2] Wuu D S, Wang W K and Horng R-H 2008 *III-Nitride devices and nanoengineering* ed Z C Feng. (Taiwan: Imperial College Press) p 462
[3] Reshchikov M A and Morkoç H 2005 *J. Appl. Phys.* **97** 061301

[4] Meneghini M, Vaccari S, Trivellin N, Dandan Z, Humphreys C, Butendheich R, Leirer C, Hahn B, Meneghesso G and Zanoni E 2012 *IEEE Trans. Electron Devices* **59** 1416
[5] Meneghini M, Trivellin N, Pavesi M, Manfredi M, Zehnder U, Hahn B, Meneghesso G and Zanoni E 2009 *Appl. Phys. Lett.* **95** 173507
[6] Breitenstein O, Bauer J, Wagner J M, Zakharov N, Blumtritt H, Lotnyk A, Kasemann M, Kwapil W and Warta W 2010 *IEEE Trans. Electron Devices* **57** 2227
[7] Veleschuk V P, Vlasenko A I, Kisselyuk M P and Lyashenko O V 2013 *J. Appl. Spectrosc.* **80** 117
[8] Chen H, Yeh Y-M, Liao C H, Lin C W, Kao C-H and Lu T-C 2013 *Microelectron. Eng.* **101** 42
[9] Chen H, Kao C-H, Lu T-C and Shei S-C 2011 *Opt. Appl.* **41** 195
[10] Cao X A, LeBoeuf S F, Kim K H, Sandvik P M, Stokes E B, Ebong A, Walker D, Kretchmer J, Lin J Y and Jiang H X 2002 *Solid-State Electron.* **46** 2291
[11] Chen N C, Wang Y N, Wang Y S, Lien W C and Chen Y C 2009 *J. Cryst. Growth* **311** 994
[12] Vanek J, Koktavy P, Dolensky J, Vesely A, Chobola Z and Paracka P 2009 *20th Int. Conf. on Noise and Fluctuations ICNF-2009AIP Conf. Proc.* 1129 641
[13] Koktavy P, Macku R, Paracka P and Krcal O 2007 *Wseas Trans. Electron.* **4** 186
[14] Kizilyalli I C, Edwards A P, Nie H., Disney D and Bour D 2013 *IEEE Trans. Electron Devices* **60** 3067
[15] Shen S C, Kao T T, Kim H J and Lee Y C etc2015 *Appl. Phys. Express* **8** 032101
[16] Boles T, Xia L, Hanson A, Kaleta A and McLean C 2014 *CS MANTECH Conf. (Denver, USA)* 321
[17] Haerle V, Hahn B, Kaiser S, Weimar A, Bader S, Eberhard F, Plössl A and Eisert D 2004 *Phys. Status Solidi a* A **201** 2736
[18] Shreter Yu G, Rebane Yu T, Zykov V A and Sidorov I G 2001 *Wide-Gap Semiconductors* (St. Petersburg: Nauka) p 125
[19] Wood C and Jena D (ed) 2008 *Polarization Effects in Semiconductors. From Ab Initio Theory to Device Applications* (New York: Springer) p 515
[20] Lee S W, Oh D C, Goto H and Ha J S etc 2006 *Appl. Phys. Lett.* **89** 132117
[21] Cao X A, Teetsov J M, D'Evelyn M P, Merfeld D W and Yan C H 2004 *Appl. Phys. Lett.* **85** 7
[22] Bertram F, Christen J, Schmidt M, Topf M, Koymov S, Fischer S and Meyer B 1997 *Mater. Sci. Eng.* B **50** 165